

ENVIRONMENTAL RESEARCH  
LETTERS

## LETTER

Assessment of radiative heating errors in Tropical Atmosphere  
Ocean array marine air temperature measurements

## OPEN ACCESS

RECEIVED  
3 March 2021REVISED  
18 November 2021ACCEPTED FOR PUBLICATION  
14 December 2021PUBLISHED  
6 January 2022

Original content from  
this work may be used  
under the terms of the  
[Creative Commons  
Attribution 4.0 licence](#).

Any further distribution  
of this work must  
maintain attribution to  
the author(s) and the title  
of the work, journal  
citation and DOI.

Francesco De Rovere<sup>1,2,\*</sup> , Davide Zanchettin<sup>1</sup> , Michael J McPhaden<sup>3</sup> and Angelo Rubino<sup>1</sup> <sup>1</sup> Ca' Foscari University of Venice, Department of Environmental Sciences, Informatics and Statistics, via Torino 155, 30172 Venezia, Mestre, Italy<sup>2</sup> Istituto di Scienze Polari, Consiglio Nazionale delle Ricerche ISP-CNR, Italy<sup>3</sup> NOAA/Pacific Marine Environmental Laboratory, 7600 Sand Point Way NE, Seattle, WA 98115, United States of America

\* Author to whom any correspondence should be addressed.

E-mail: [francesco.derovere@unive.it](mailto:francesco.derovere@unive.it)**Keywords:** radiative heating error, marine air temperature measurements, Tropical Atmosphere Ocean Array, Global Tropical Moored Buoy ArraySupplementary material for this article is available [online](#)**Abstract**

We assess the radiative heating error affecting marine air temperature (MAT) measurements in the Tropical Atmosphere Ocean array. The error in historical observations is found to be ubiquitous across the array, spatially variable and approximately stationary in time. The error induces spurious warming during daytime hours, but does not affect night-time temperatures. The range encompassing the real, unknown daily- and monthly-mean values is determined using daytime and night-time mean temperatures as upper and lower limits. The uncertainty in MAT is less than or equal to 0.5 °C and 0.2 °C for 95% of daily and monthly estimates, respectively. Uncertainties impact surface turbulent heat flux estimates, with potentially significant influences on the quantification of coupled ocean-atmosphere processes.

**1. Introduction**

The Tropical Atmosphere Ocean (TAO) array consists of about 70 moorings in the Tropical Pacific Ocean acquiring high-frequency meteorological and oceanographic data (McPhaden 1995, McPhaden *et al* 1998). Since its advent in 1985, the TAO array has become the major source of *in situ* measurements for the investigation of near-surface atmospheric and oceanographic processes in the equatorial Pacific. The success of the TAO project fostered the development of two additional arrays in the Atlantic and Indian oceans, namely the Prediction and Research Moored Array in the Atlantic (PIRATA, Bourlès *et al* 2019) and the Research Moored Array for African-Asian-Australian Monsoon Analysis and Prediction (RAMA, McPhaden *et al* 2009), respectively. The three arrays constitute the Global Tropical Moored Buoy Array (GTMBA) and share the same buoy and sensor instrumentation (McPhaden *et al* 2010). GTMBA data are widely used to analyse regional climatic phenomena, e.g. the El Niño-Southern Oscillation in the equatorial Pacific (McPhaden *et al* 2020) and the Indian Ocean Dipole in the Indian

Ocean (McPhaden *et al* 2015), to contribute to global observational datasets and observing systems (e.g. HadCRUT, ICOADS, GOOS and GCOS), to validate satellite observations and to evaluate climate model output (Good *et al* 2020). The temperature sensors mounted on GTMBA buoys are known to be susceptible to a radiative heating error (RHE), which hampers the reliability of near-surface marine air temperature (MAT) measurements. However, only few studies have systematically assessed RHE on moorings and, to our knowledge, none has systematically assessed the impact of the RHE on TAO data. In the present investigation we address this gap and discuss implications of the RHE for the quantification of daily and monthly MAT variability over the tropical Pacific Ocean.

On GTMBA buoys, MAT measurements are made by Pt-100 RTD (resistance temperature detector) sensors covered with naturally ventilated radiation shields. A shield is composed of ten plates made of white polyvinyl chloride placed one above the other protecting the sensor from direct solar radiation, precipitation and spray from wave breaking. The shield is designed to allow for air flow through

the plates and for convective cooling. Thus, a net heat loss is induced, which should equal the solar heating (Gill 1983). The accuracy of such MAT measurements was originally questioned by Anderson and Baumgartner (1998), hereafter referred to as AB1998, who revealed the RHE in measurements obtained by buoys deployed within the TOGA/COARE monitoring program (Webster and Lukas 1992, Weller and Anderson 1996). The error was detected by comparing air temperature measurements obtained from a sensor covered by a naturally ventilated radiation shield originally mounted on the TOGA/COARE buoys and a sensor examining the air within an actively ventilated radiation shield working only in daylight hours installed on the same buoy. The shape of the mean diurnal cycle of MAT was found to differ significantly between the two sources during daylight hours. The ‘aspirated’ temperature constantly increases from 06 h to 12–15 h local time, showing only one peak throughout the day, while the ‘naturally ventilated’ diurnal evolution features two peaks occurring around mid-morning and mid-afternoon, revealing that, because of shield geometry, a sensor’s spurious heating occurs, which is maximum with a Sun elevation between  $40^\circ$  and  $70^\circ$ . This RHE was explained by excess heating of the air temperature inside the shield caused by solar radiation and insufficient air recirculation. However, the limited number of observations used in AB1998 and the currently large TAO dataset requires an updated assessment of the RHE.

Existing correction models for the RHE build on consideration of the shield heat budget (AB1998) and on synchronous acquisition of solar radiation and wind speed (Nakamura and Mahrt 2005). Models rely on the comparison between the erroneous and the accurate air temperature measurements to estimate their parameters, which depends on the specific characteristics of each sensor. AB1998 estimated these empirical parameters using measurements spanning only a few days from just a few buoys; whether they are generally applicable is an open question. Moreover, the operating periods of the different sensors mounted on each TAO buoy are typically not synchronous. Hence, wind speed and solar radiation measurements are not always available during the whole MAT observational period and the correction cannot be always applied.

In this work we focus on daily and monthly mean values to address the following scientific question: given that MAT measurements from the TAO array are affected by a variable RHE, is it possible to constrain the true MAT evolution over decades of measurements from tens of buoys within a reliable uncertainty range? We proceed as follows. First, the ubiquitous presence of the RHE among the TAO buoys is determined by qualitatively comparing their average MAT diurnal cycle with the ‘erroneous’ diurnal cycle described by AB1998. Then, the

uncertainty associated with the RHE in the daily and monthly MAT estimates from the TAO array is assessed by comparing ‘all-day’ and ‘night-time’ average values (adMAT and nMAT, respectively). We identify the interval containing the true values by assuming that, for any given day or month, the true daily average value is smaller than the adMAT estimate and larger than the nMAT estimate. This assumption builds on the RHE being positive and always adding to the observed MAT during daylight hours, resulting in a warmer observed MAT mean compared to the true MAT mean (AB1998). Accordingly, the observed adMAT estimate sets an upper boundary to the true value. The lower boundary is set by the nMAT estimate, which is calculated over the coolest hours of the day not affected by the RHE, given the obvious lack of direct solar radiation during night time. Days or months may occasionally feature larger MAT values during night-time hours due to rapid modifications in local meteorological conditions as the passage of a storm, which can cause a quick drop in daytime temperatures. In this case, the true MAT value cannot be enclosed within two limits and we therefore exclude these days and months from the analysis. Accordingly, the difference between adMAT and nMAT, hereafter referred to as  $\Delta$ , quantifies the interval inclusive of the true adMAT (daily or monthly) value. By definition  $\Delta$  will be always positive as negative values are excluded from the analysis.

In the main analysis, scatterplots are used to compare the distribution of  $\Delta$  according to adMAT for both daily and monthly estimates. The spatio-temporal variation of  $\Delta$  in the TAO array is investigated by inspecting the temporal mean and standard deviation of  $\Delta$  as well as the  $\Delta$  variation in time among the TAO buoys. We also examine how the uncertainty in MAT measurements due to the RHE propagates to estimates of local surface turbulent sensible ( $F_h$ ) and latent ( $F_q$ ) heat fluxes.

## 2. Materials and methods

This study utilizes all 10 min MAT data acquired by the TAO and GTMBA arrays from the end of the 90s to the end of 2020 (see figure S1 (available online at [stacks.iop.org/ERL/17/014040/mmedia](https://stacks.iop.org/ERL/17/014040/mmedia)) for data availability). Note that only buoys positioned eastward of  $165^\circ$  E acquire 10 min observations. Then, data are used to assess the interval  $\Delta$  inclusive of the true MAT value, for daily and monthly estimates.

The presence of the RHE in GTMBA data is inspected through the MAT mean diurnal cycle, obtained by averaging MAT diurnal anomalies. Diurnal anomalies are defined as deviations of instantaneous measurements throughout a day from the average of all such measurements, i.e. the daily average. Anomalies are computed over a 24 h period to remove the effect of longer-term variability. Therefore, processes responsible for diurnal variability are

highlighted. The MAT mean diurnal cycle is obtained by averaging diurnal anomalies throughout the day, from 00 h to 23.50 h local time, at the available sampling frequency of 10 min. Hereafter, all times are reported in local time.

Daily adMAT, nMAT and  $\Delta$  are defined as follows:

$$\text{(Daily) adMAT}_i = \frac{\sum_j \text{MAT}_{i,j}}{n}$$

$$\text{(Daily) nMAT}_i = \frac{\sum_k \text{MAT}_{i,k}}{n}$$

$$\text{(Daily) } \Delta_i = \text{adMAT}_i - \text{nMAT}_i$$

where  $i$  is one specific day,  $j$  indicates all 10 min timings between 00 h and 24 h in day  $i$ ,  $k$  indicates those 10 min timings within the 00–05 h and 19–24 h intervals in day  $i$ , and  $n$  the number of measurements utilised in the calculations, 144 for adMAT and 48 for nMAT. We chose these conservative time intervals to exclude any measurement acquired during sunlight hours, since sunrise and sundown occur approximately at 06 h and 18 h near the equator.

Monthly adMAT, nMAT and  $\Delta$  are defined as follows:

$$\text{(Monthly) adMAT}_l = \frac{\sum_m \text{MAT}_{l,m}}{n}$$

$$\text{(Monthly) nMAT}_l = \frac{\sum_p \text{MAT}_{l,p}}{n}$$

$$\text{(Monthly) } \Delta_l = \text{adMAT}_l - \text{nMAT}_l$$

where  $l$  is one specific month,  $m$  indicates all 10 min timings between 00 h and 24 h in month  $l$ ,  $p$  indicates those 10 min timings within the 00–05 h and 19–24 h intervals in month  $l$ , and  $n$  the number of measurements utilised in each calculation. In calculating daily and monthly averages, no precautions were taken to exclude those days/months with an excessive number of missing observations.

Negative  $\Delta$  are excluded from the analysis (see figure S1 reporting percentages of excluded data for each TAO buoy). We found that these negative  $\Delta$  days are largely associated with low insolation conditions (not shown). Therefore, given the dependence of the RHE on solar radiation, the adMAT estimates associated to negative  $\Delta$  are likely to be very close to the true values. We note that, theoretically, some cases in which the observed  $\Delta$  is positive even though the true  $\Delta$  is negative can occur, which would prevent the correct estimation of the interval encompassing the true daily or monthly MAT average using our methodology. These cases require the true daylight MAT average to be smaller than the corresponding true nMAT average with strongly perturbed meteorological conditions during daytime that would lower

MAT during daylight hours and totally damp the RHE. As a consequence, these cases would be classified as days with negative  $\Delta$  and excluded from the analysis. However, without independent accurate measurements of MAT, we cannot identify all the true negative  $\Delta$  cases and hence ascertain whether they are completely excluded from the present analysis. A comparison between ERA5 hourly air temperature data and TAO MAT data at selected buoy locations reveals that the percentage of days featuring negative  $\Delta$  is very similar among the two datasets and generally larger for TAO. On the other hand, for monthly estimates almost no such cases are detected in either dataset (not shown). Therefore, we acknowledge that our results are more robust for monthly estimates compared to daily estimates, though the latter still provide useful guidance on the magnitude of the RHE.

The variation of  $\Delta$  according to adMAT daily and monthly estimates is examined through 2D density plots. Five different quantiles of the  $\Delta$  distribution observed within single adMAT intervals of 0.05 °C are calculated. Selected quantiles are 0.995 ( $Q_{0.995}$ ), 0.95 ( $Q_{0.95}$ ), 0.9 ( $Q_{0.9}$ ), 0.8 ( $Q_{0.8}$ ).  $\Delta$  quantiles are calculated only for those adMAT intervals containing at least five values. A relation linking monthly  $\Delta$  to adMAT is inferred by fitting different polynomial regressions up to the 4th order to each selected  $\Delta$  quantile using adMAT as predictor. One model for each  $\Delta$  quantile is selected according to the Akaike Information Criterion (AIC). Spatio-temporal variations of  $\Delta$  are assessed by reporting average, standard deviation and linear trend of  $\Delta$  calculated for the whole time series at each buoy.  $\Delta$  standard deviations for the whole TAO array are reported using a min-max normalisation.

$F_h$  and  $F_q$  are estimated using the algorithm proposed by Zeng *et al* (1998) and developed by Winslow *et al* (2016).  $F_h$  and  $F_q$  are estimated using daily and monthly adMAT and nMAT, relative humidity (RH), sea-surface temperature (SST), wind speed and sea-level pressure (SLP) from the TAO array. RH is calculated through MAT, thus we differentiate adRH and nRH as for adMAT and nMAT. A constant value (1013 mb) is used for SLP since observations are not available at all buoys. Estimates of fluxes using Zeng's algorithm and by PMEL (Fairall *et al* 2003) are compared for few sample buoys in figure S2.  $\Delta F_h$  and  $\Delta F_q$  are defined as the difference between the all-day and night-time estimates of  $F_h$  and  $F_q$ , respectively. We examine the mean and standard deviation of  $\Delta F_h$  and  $\Delta F_q$  for all TAO buoys. In addition, the relation between adMAT and heat fluxes is examined through a 2D density plot of  $\Delta F_q/F_q$  and  $\Delta F_h/F_h$  versus adMAT to see how uncertainties in  $F_q$  and  $F_h$  grows in relation to adMAT.

TAO instrumental errors and how these relate to our analysis are discussed as follows. There are two sources of error in the TAO MAT measurements,

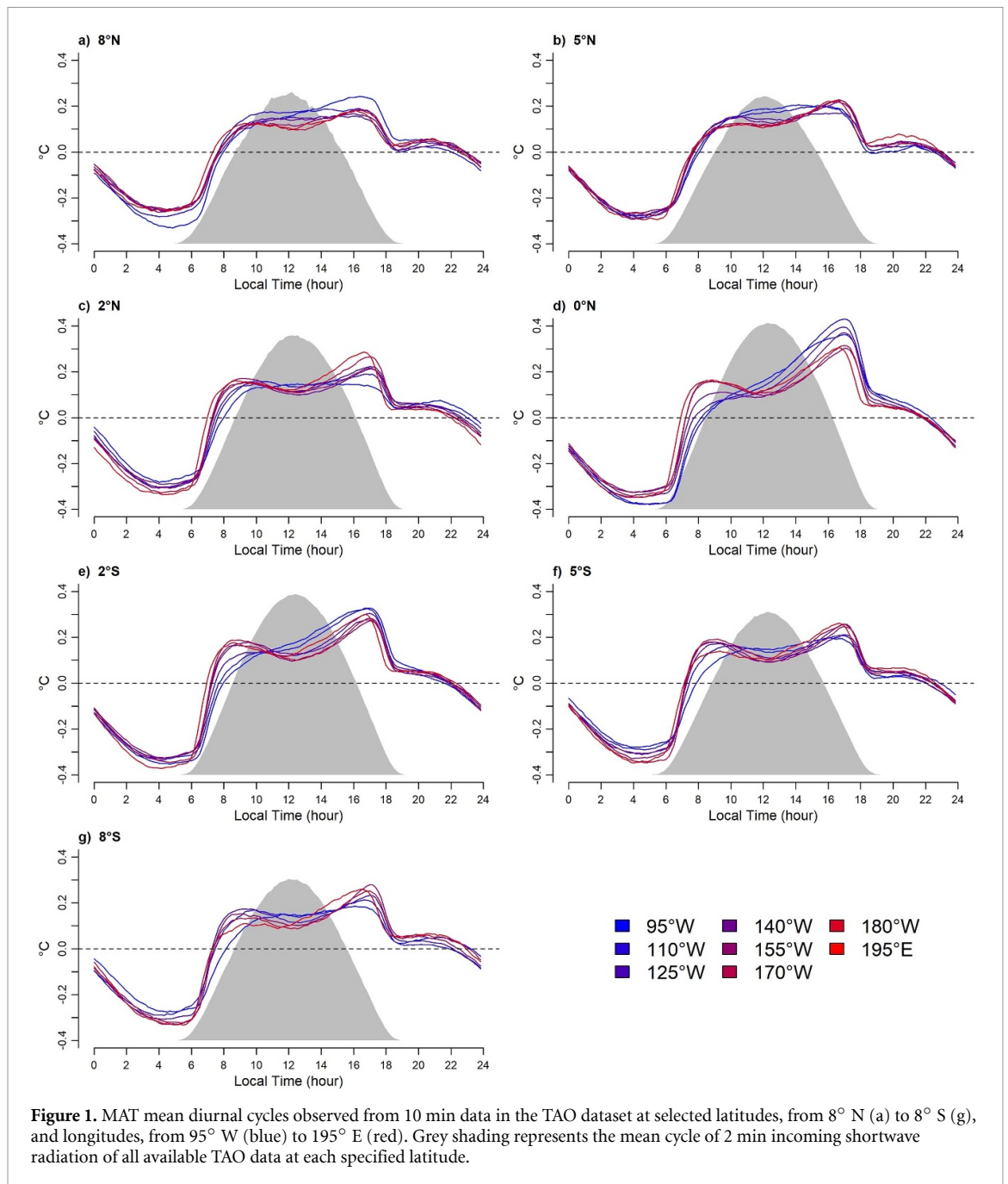


**Figure 1.** MAT mean diurnal cycles observed from 10 min data in the TAO dataset at selected latitudes, from 8° N (a) to 8° S (g), and longitudes, from 95° W (blue) to 195° E (red). Grey shading represents the mean cycle of 2 min incoming shortwave radiation of all available TAO data at each specified latitude.

apart from the RHE: (a) general instrumental error; (b) geophysical noise from high frequency random fluctuations in the 10 min data. The instrumental error (a) is on the order of 0.1 °C and 0.2 °C for an individual sensor, depending on mooring type. Details can be found at [www.pmel.noaa.gov/gtmba/sensor-specifications](http://www.pmel.noaa.gov/gtmba/sensor-specifications) and in Lake *et al* (2003). This error is related to sensor calibration drift over a year-long deployment. Crucially for our study, since this instrumental error is related primarily to calibration drift, it will be nearly identical for adMAT and nMAT over a 24 hour period. So the difference between these two measures, i.e.  $\Delta$ , largely eliminates this noise error, such that at most it should be an order of magnitude smaller than the error for an individual sensor. Thus,  $\Delta$  estimates greater than

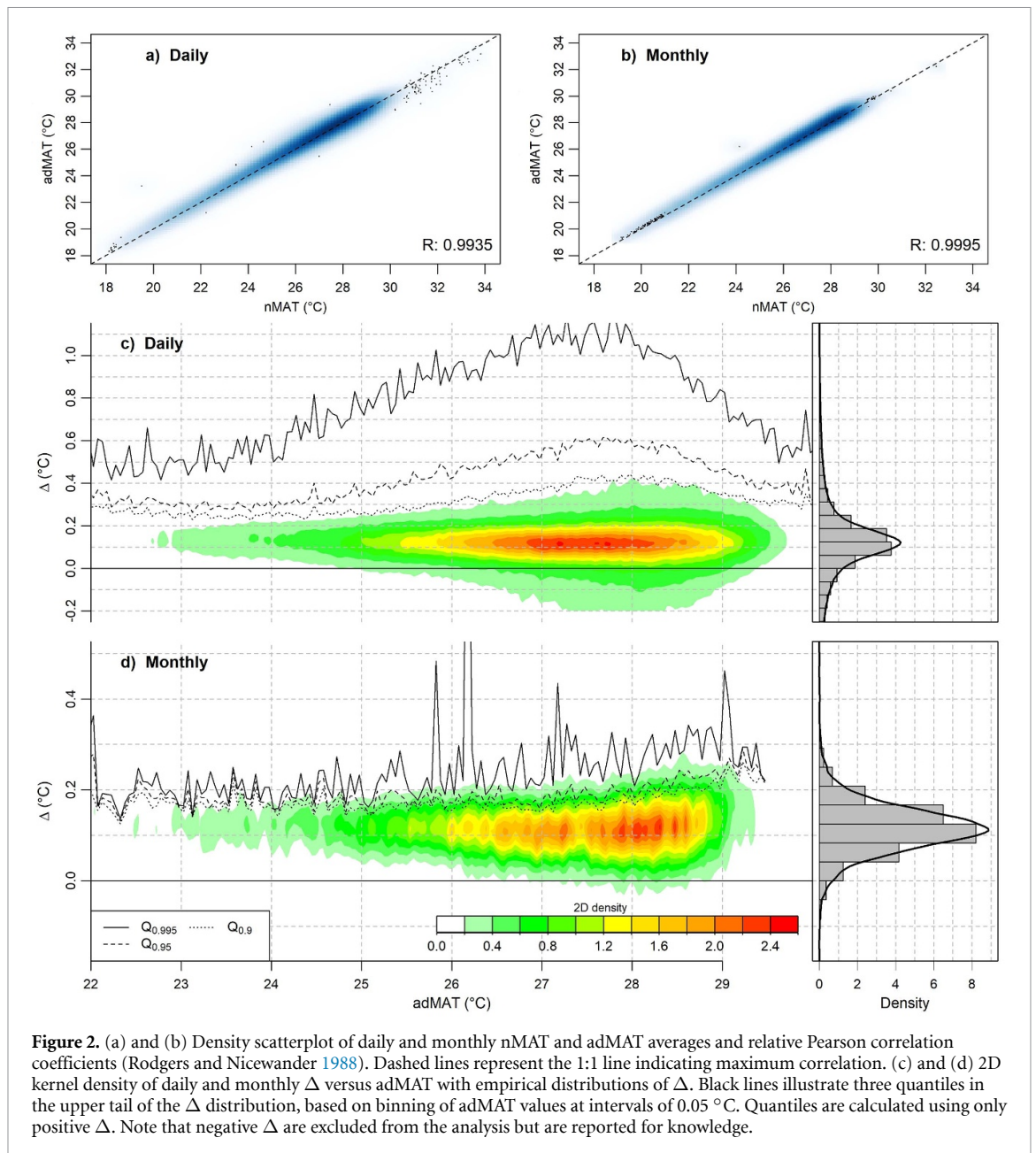
about 0.01 °C and 0.02 °C will be much more influenced by the RHE than by instrumental errors resulting from calibration drift over time. The geophysical noise based on individual 10 min samples (b) is random and so is reduced by temporal/spatial averaging. Reduction in this noise is one reason for the difference in the results between the monthly and daily statistics.

### 3. Results and discussion

#### 3.1. The RHE in the TAO array

Figure 1 displays the MAT mean diurnal cycles for selected TAO buoys grouped by latitude.

A double-peak evolution is present at every buoy. MAT starts to warm around 6 h, when solar radiation begins to rise, and reaches its maximum around



17 h. However, MAT does not rise monotonically: a period featuring stable or even decreasing temperatures occurs between 9 h and 12 h. In the afternoon, MAT decreases sharply between 17 h and 18 h and then more regularly until 3 h. Finally, MAT remains almost stable between 3 h and 6 h. Therefore, two relative peaks occur throughout the 24 hour period, one around 8 h and the other around 17 h. Figure S3 reports a very similar behaviour in PIRATA and RAMA buoys. The presence of a double-peak cycle contrasts with the expected occurrence of a single daily maximum of near-surface air temperature a few hours after 12 h following from the varying sun inclination and sharing similarities with the SST diurnal cycle (Kawai and Wada 2007, Morak-Bozzo *et al* 2016). It is instead consistent with the shape and time of the RHE illustrated by AB1998. Hence, the GTMBA measurements of air temperature

are ubiquitously affected by the RHE. The two MAT daily peaks are found to be greatest along the equator. The small variations observed among buoys are likely due to distinct predominant insolation and wind conditions, which differently affect the MAT diurnal cycle. Different positions of the buoys relative to the boundaries of local time zones may cause the shifts between mean diurnal cycle observed at different longitudes.

### 3.2. $\Delta$ assessment in adMAT data

The identification of the RHE motivates an assessment of how it affects daily-mean and monthly-mean estimates of MAT. The range constraining the true (unobserved) MAT mean is defined as  $\Delta$  and includes the erroneous adMAT observed value as upper limit and the nMAT value as lower limit. This approach is viable as far as  $\Delta$  is relatively small

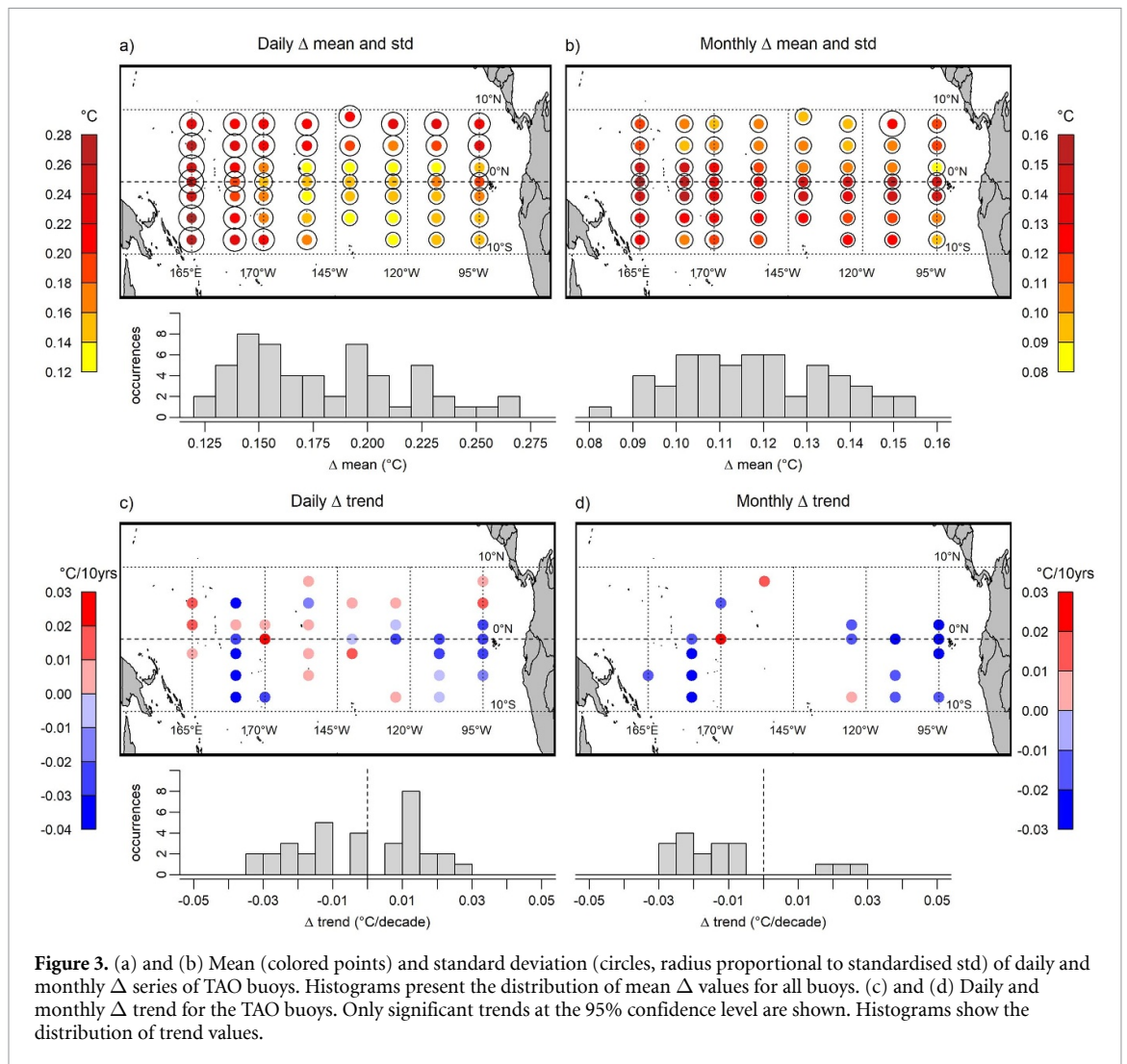
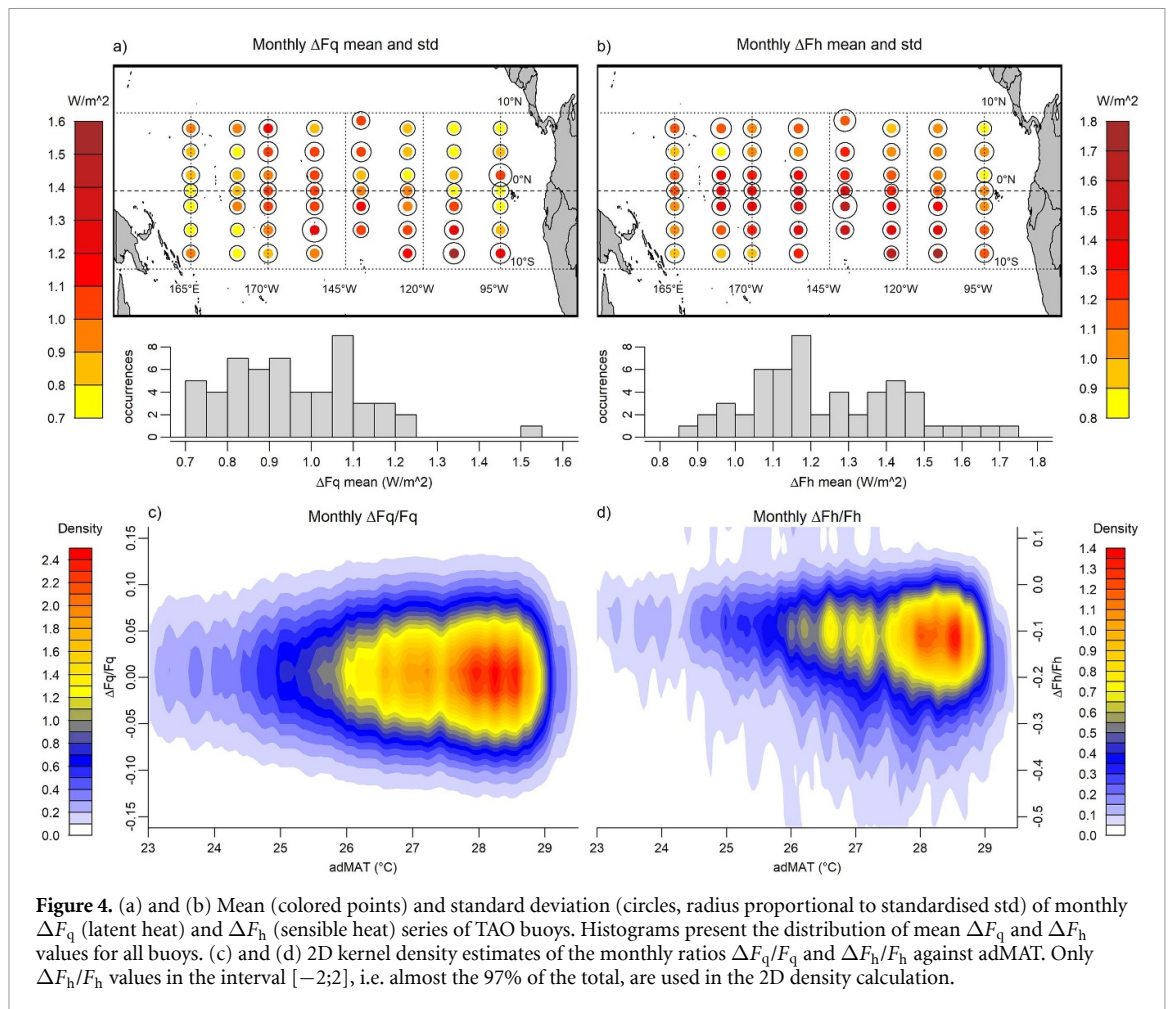


**Figure 3.** (a) and (b) Mean (colored points) and standard deviation (circles, radius proportional to standardised std) of daily and monthly  $\Delta$  series of TAO buoys. Histograms present the distribution of mean  $\Delta$  values for all buoys. (c) and (d) Daily and monthly  $\Delta$  trend for the TAO buoys. Only significant trends at the 95% confidence level are shown. Histograms show the distribution of trend values.

so as not to mask the observed adMAT variability. Practically, the ratio between mean  $\Delta$  and the adMAT standard deviation must be small. For individual buoys in the TAO array, values of this ratio are all below 0.35 for both daily and monthly data, the latter typically ranging between 0.05 and 0.20 (see figure S4).

An almost perfect linear relation exists between adMAT and nMAT for daily as well as monthly data from TAO buoys (figures 2(a) and (b)). adMAT values are slightly above the 1:1 line, revealing that adMAT averages are often a few tenths of degree higher than nMAT averages. The 95% of positive  $\Delta$  values are confined within the 0 °C–0.5 °C interval for daily and within the 0 °C–0.2 °C interval for monthly estimates (figures 2(c) and (d)). Quantiles in the upper tail of the  $\Delta$  distribution show a different behaviour between daily and monthly values. For daily estimates, the  $\Delta$  distribution conditioned to adMAT values remains rather constant for adMAT values below  $\sim 24$  °C, then it substantially enlarges as adMAT approaches 27 °C and 28 °C to narrow again toward the observed warmest adMAT values (see the

$Q_{0.995}$  and  $Q_{0.95}$  lines in figure 2(c)). Conversely, for monthly estimates, the rather flat  $Q_{0.995}$  and  $Q_{0.95}$  lines indicate that the  $\Delta$  distribution is independent of adMAT until the latter reaches  $\sim 27$  °C, where the  $\Delta$  distribution progressively enlarges (figure 2(d)). Monthly data yield almost always positive  $\Delta$  values, indicating that nMAT is a robust lower limit for the true adMAT value. This allows skillful application of simple regression models to estimate an interval encompassing the true values of monthly adMAT depending on the adMAT estimates themselves. Table S1 reports the parameters of polynomial regression models up to the fourth order featuring the lowest AIC value for each  $\Delta$  monthly quantile. Table S2 reports the AIC values for each fitted model. Fits are graphically reported in figure S5. Both skill and order of the regression model increase with the considered quantile, with a maximum explained variance of about 28% for  $Q_{0.995}$  obtained from a 4th order polynomial. Note that using a high quantile to define the upper threshold for the real adMAT value corresponds to setting a very conservative uncertainty range.



### 3.3. $\Delta$ spatio-temporal assessment

Figure 3 reports  $\Delta$  mean, standard deviation (std) and temporal trend for the selected TAO buoys. See figure S6 for the full  $\Delta$  temporal evolution for three sample buoys.

The mean  $\Delta$  values range between 0.12 °C and 0.28 °C for daily estimates and between 0.07 °C and 0.16 °C for monthly estimates, confirming that monthly  $\Delta$  values are generally smaller than daily ones. Daily  $\Delta$  means and standard deviations are smaller in the central and south-eastern equatorial Pacific and higher in the western and northernmost portion of the TAO array. This pattern corresponds well with the spatial distribution of mean rainfall and wind speed in the tropical Pacific, the former with higher values in the western Pacific, the Intertropical Convergence Zone and the South Pacific Convergence Zone, the latter with larger velocities concentrated in the central and southern Pacific (see figure S7). In contrast, monthly  $\Delta$  statistics vary without a clear large-scale spatial pattern, except for larger mean values along the equator and smaller values in the northernmost portion of the array.  $\Delta$  trends encompass positive and negative values, and do not display spatial patterns clearly linked to known large-scale phenomena in the area (figures 3(c) and (d)). In contrast to  $\Delta$  mean and standard deviation,  $\Delta$

trend yields similar results for daily and monthly data. Toward the goal of using  $\Delta$  to constrain the range of true adMAT values,  $\Delta$  trends, although significant in many buoys, are one order of magnitude smaller than the corresponding mean values (see figure 2) and appear to be non-systematic. Thus,  $\Delta$  does not vary significantly through time in the TAO dataset, suggesting that no physical process beyond the RHE affects the difference between the all-day and night-time estimates. We conclude that our statistical models linking the RHE to the adMAT are reliable throughout the analyzed period. Moreover,  $\Delta$  trends are at least one order of magnitude smaller than adMAT trend estimates (see figure S8), thus suggesting that  $\Delta$  do not significantly influence MAT long-term trends.

### 3.4. RHE and heat flux estimates

We examine how  $\Delta$  affects the daily (figure S9) and monthly (figure 4) estimates of local sensible and latent heat surface fluxes.

Figure 4 shows that the mean values of  $\Delta F_q$  and  $\Delta F_h$  calculated using monthly estimates of adMAT and nMAT span similar ranges, which never exceed 1.8 W m<sup>-2</sup> for both variables. Conversely, when daily estimates of adMAT and nMAT are used,  $\Delta F_q$  and  $\Delta F_h$  reach 6.0 and 2.4 W m<sup>-2</sup>, respectively.

The geographical pattern of the monthly  $\Delta F_h$  mean resembles that of  $\Delta$  reported in figure 3(a), suggesting that  $F_h$  depends on MAT more than  $F_q$  as one might expect. Figures 4(c) and (d) illustrate the relative magnitude of monthly  $\Delta F_q$  and  $\Delta F_h$  compared to the  $F_q$  and  $F_h$  estimates, respectively, for all buoys. The distribution of  $\Delta F_q$  is rather symmetric around zero, with the vast majority of the estimates between  $-0.05$  and  $0.05$  and only 1% of the absolute values exceeding  $0.065$ . Therefore, uncertainty in  $F_q$  due to uncertainty in the MAT estimates is generally negligible compared to the true value of  $F_q$ . Instead, MAT uncertainty leads to larger uncertainties in monthly  $F_h$ , with almost 10% of the absolute estimates greater than  $0.7$ , often broadly exceeding  $1.0$ . However, these large  $\Delta F_h/F_h$  ratios are mainly associated to small  $F_h$  estimates. Excluding  $F_h$  estimates smaller than  $2 \text{ W m}^{-2}$  (10% of the total) results in only the 1.5% of the absolute  $\Delta F_h/F_h$  values being greater than  $0.7$ . Data indicate a systematic underestimation of the true  $F_h$  value since  $F_h$  estimates are largely positive (86% of the total estimates) whereas  $\Delta F_h/F_h$  have predominantly negative values. Compared to monthly estimates, daily estimates present a similar behaviour even though the relative importance of  $\Delta F_q$  and  $\Delta F_h$  are slightly more pronounced (see figure S9). Across the whole adMAT range, both daily and monthly relative magnitudes of  $\Delta F_q$  are much more uniform compared to  $F_h$ .

#### 4. Conclusions

Daytime MAT measurements acquired with naturally ventilated shields instruments are affected by an error due to radiative heating. The RHE reshapes the diurnal MAT cycle by adding spurious warming for low angles of incoming solar radiation that yields a double-peaked daily MAT cycle, a feature shared by all GTMBA buoys gathering 10 min data. An accurate quantification of the RHE requires comparing naturally ventilated shield observations against a parallel set of truthful MAT measurements. This is not possible for currently available MAT data. To overcome this limitation, a simple approach to determine the range of daily- and monthly-mean values encompassing the real MAT average value for the TAO array is proposed. Under the assumption that the RHE does not affect observations from 19 h to 5 h local time and the average of all-day observations be larger than that of night-time observations, the true average value is enclosed within the interval  $[\text{mean}(n\text{MAT}), \text{mean}(\text{adMAT})]$  of modulus equal to  $\Delta$ .

We found that this interval, based on the 95-percentile range of data, is always smaller than  $0.5 \text{ }^\circ\text{C}$  for the daily and  $0.2 \text{ }^\circ\text{C}$  for the monthly estimates. Given the dependency of  $\Delta$  on adMAT, regression models with different accuracies are provided as a simple way to evaluate the uncertainty of past adMAT monthly estimates. Our methodology will incorrectly

estimate  $\Delta$  when the observed value is positive but the true value is negative. However, we are confident that the vast majority of cases with a true negative  $\Delta$  correspond to those with an observed negative  $\Delta$ , which we have excluded from the main analysis. Still, our methodology is more robust for monthly estimates compared to daily estimates because of this uncertainty.

The trend analysis of  $\Delta$  reveals no significant or very small changes in time, suggesting that our statistical models are robust throughout the period of study and that  $\Delta$  does not influence MAT long-term trends. The uncertainty in MAT values propagates differently into surface sensible and latent heat fluxes. Differences between all-day and night-time monthly estimates of latent heat fluxes are generally small (less than 7% for most of the estimates), while differences increase for the sensible heat fluxes (over 70% for 10% of estimates). Fortunately, sensible heat fluxes are generally smaller than latent heat fluxes in the tropics, though the relative errors are still potentially significant in terms of coupled ocean-atmosphere processes.

Our analysis has focused on MAT data collected from moored buoys of the TAO array in the Pacific Ocean. However, as noted in the introduction, PIRATA moorings in the tropical Atlantic and RAMA moorings in the tropical Indian Ocean are of a similar design with instrumentation identical to that used in TAO. Thus, the key results of this study will apply to moored MAT data collected in PIRATA and RAMA even though not explicitly included in our analysis.

#### Data availability statement

The data that support the findings of this study are openly available at the following URL/DOI: [www.pmel.noaa.gov/gtmba/](http://www.pmel.noaa.gov/gtmba/).

#### Acknowledgments

MJM is supported by NOAA. PMEL contribution No. 5103. The authors thank the anonymous reviewers for their helpful comments.

#### ORCID iDs

Francesco De Rovere  <https://orcid.org/0000-0002-0945-5584>

Davide Zanchettin  <https://orcid.org/0000-0001-5929-6983>

Michael J McPhaden  <https://orcid.org/0000-0002-8423-5805>

Angelo Rubino  <https://orcid.org/0000-0003-3857-4811>

#### References

Anderson S P and Baumgartner M F 1998 Radiative heating errors in naturally ventilated air temperature measurements made from buoys *J. Atmos. Ocean. Technol.* **15** 157–73

- Bourlès B et al 2019 PIRATA: a sustained observing system for tropical Atlantic climate research and forecasting *Earth Space Sci.* **6** 577–616
- Fairall C W, Bradley E F, Hare J E, Grachev A A and Edson J B 2003 Bulk parameterization of air–sea fluxes: updates and verification for the COARE algorithm *J. Clim.* **16** 571–91
- Gill G C 1983 Comparison testing of selected naturally ventilated solar radiation shields (NOAA Data Buoy Office Rep. (Bay St. Louis, MS, in partial fulfillment of Contract NA-82-0A-A-266) p 38 (available at: <https://repository.library.noaa.gov/view/noaa/6542>)
- Good P, Chadwick R, Holloway C E, Kennedy J, Lowe J A, Roehrig R and Rushley S S 2020 High sensitivity of tropical precipitation to local sea-surface temperature *Nature* **589** 408–14
- Kawai Y and Wada A 2007 Diurnal sea surface temperature variation and its impact on the atmosphere and ocean: a review *J. Oceanogr.* **63** 721–44
- Lake B J, Noor S M, Freitag H P and McPhaden M J 2003 Calibration procedures and instrumental accuracy estimates of ATLAS air temperature and relative humidity measurements NOAA Tech. Memo. OAR PMEL-123 NOAA/Pacific Marine Environmental Laboratory (Seattle, WA: University of Washington, Joint Institute for the Study of the Atmosphere and Ocean) p 23 (available at: <https://repository.library.noaa.gov/view/noaa/11034>)
- McPhaden M J et al 1998 The tropical ocean–global atmosphere (TOGA) observing system: a decade of progress *J. Geophys. Res.* **103** 14169–240
- McPhaden M J, Ando K, Bourlès B, Freitag H P, Lumpkin R, Masumoto Y and Voustden D 2010 The global tropical moored buoy array *Proc. Ocean Obs.* **9** 668–82
- McPhaden M J, Lee T, Fournier S and Balmaseda M A 2020 ENSO observations *El Niño Southern Oscillation in a Changing Climate* Geophysical Monograph Series (Hoboken, NJ: John Wiley & Sons, Inc and American Geophysical Union) pp 39–63
- McPhaden M J, Meyers G, Ando K, Masumoto Y, Murty V S N, Ravichandran M, Syamsudin F, Vialard J, Yu L and Yu W 2009 RAMA: the research moored array for African–Asian–Australian monsoon analysis and prediction *Bull. Am. Meteorol. Soc.* **90** 459–80
- McPhaden M J, Wang Y and Ravichandran M 2015 Volume transports of the Wyrtki jets and their relationship to the Indian Ocean Dipole *J. Geophys. Res.: Oceans* **120** 5302–17
- McPhaden M 1995 The tropical atmosphere and ocean (TAO) array is completed *Bull. Am. Meteorol. Soc.* **76** 731–9
- Morak-Bozzo S, Merchant C J, Kent E C, Berry D I and Carella G 2016 Climatological diurnal variability in sea surface temperature characterized from drifting buoy data *Geosci. Data J.* **3** 20–28
- Nakamura R and Mahrt L 2005 Air temperature measurement errors in a naturally ventilated multi-plate radiation shield *J. Atmos. Oceanic Technol.* **22** 1046–58
- Rodgers J L and Nicwander W A 1988 Thirteen ways to look at the correlation coefficient *Am. Stat.* **42** 59–66
- Webster P J and Lukas R 1992 TOGA COARE: the coupled ocean–atmosphere response experiment *Bull. Am. Meteorol. Soc.* **73** 1377–416
- Weller R A and Anderson S P 1996 Surface meteorology and air–sea fluxes in the western equatorial Pacific warm pool during the TOGA Coupled Ocean–Atmosphere Response Experiment *J. Clim.* **9** 1959–90
- Winslow L A, Zwart J A, Batt R D, Dugan H A, Woolway R I, Corman J R, Hanson P C and Read J S 2016 LakeMetabolizer: an R package for estimating lake metabolism from free-water oxygen using diverse statistical models *Inland Waters* **6** 622–36
- Zeng X, Zhao M and Dickinson R E 1998 Intercomparison of bulk aerodynamic algorithms for the computation of sea surface fluxes using TOGA COARE and TAO data *J. Clim.* **11** 2628–44